RADC-TR-89-290
In-House Report
November 1989

PICOSECOND LASER FACILITY

Dorothy Jackson, 1Lt, USAF and Michael Ward, 1Lt, USAF

APPROVED FOR PUBLIC RELEASE; DISTRIBUTION UNLIMITED.

ROME AIR DEVELOPMENT CENTER
Air Force Systems Command
Griffiss Air Force Base, NY 13441-5700

This report has been reviewed by the RADC Public Affairs Office (PA) and is releasable to the National Technical Information Service (NTIS). At NTIS it will be releasable to the general public, including foreign nations.

RADC TR-89-290 has been reviewed and is approved for publication.

APPROVED: 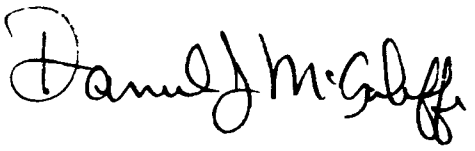

DANIEL J. McAULIFFE
Chief, Telecommunications Division
Directorate of Communications

APPROVED:

JOHN A. GRANIERO
Technical Director
Directorate of Communications

FOR THE COMMANDER:

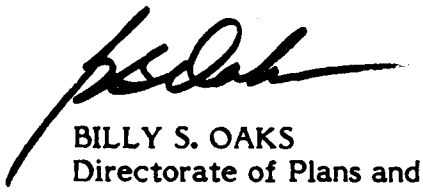

BILLY S. OAKS
Directorate of Plans and Programs

If your address has changed or if you wish to be removed from the RADC mailing list, or if the addressee is no longer employed by your organization, please notify RADC (DCLW) Griffiss AFB NY 13441-5700. This will assist us in maintaining a current mailing list.

Do not return copies of this report unless contractual obligations or notices on a specific document requires that it be returned.

UNCLASSIFIED

SECURITY CLASSIFICATION OF THIS PAGE

REPORT DOCUMENTATION PAGE

Form Approved OMB No. 0704-0188

1a. REPORT SECURITY CLASSIFICATION: UNCLASSIFIED	1b. RESTRICTIVE MARKINGS: N/A
2a. SECURITY CLASSIFICATION AUTHORITY: N/A	3. DISTRIBUTION/AVAILABILITY OF REPORT: Approved for public release; distribution unlimited.
2b. DECLASSIFICATION/DOWNGRADING SCHEDULE: N/A	
4. PERFORMING ORGANIZATION REPORT NUMBER(S): RADC-TR-89-290	5. MONITORING ORGANIZATION REPORT NUMBER(S): N/A
6a. NAME OF PERFORMING ORGANIZATION: Rome Air Development Center; 6b. OFFICE SYMBOL (If applicable): DCLW	7a. NAME OF MONITORING ORGANIZATION: Rome Air Development Center (DCLW)
6c. ADDRESS (City, State, and ZIP Code): Griffiss AFB NY 13441-5700	7b. ADDRESS (City, State, and ZIP Code): Griffiss AFB NY 13441-5700
8a. NAME OF FUNDING/SPONSORING ORGANIZATION: Rome Air Development Center; 8b. OFFICE SYMBOL (If applicable): DCLW	9 PROCUREMENT INSTRUMENT IDENTIFICATION NUMBER: N/A
8c. ADDRESS (City, State, and ZIP Code): Griffiss AFB NY 13441-5700	10. SOURCE OF FUNDING NUMBERS: PROGRAM ELEMENT NO. 63726F; PROJECT NO. 4519; TASK NO 21; WORK UNIT ACCESSION NO. TK

11. TITLE (Include Security Classification): PICOSECOND LASER FACILITY

12. PERSONAL AUTHOR(S): Dorothy Jackson, 1Lt, USAF and Michael Ward, 1Lt, USAF

13a. TYPE OF REPORT	13b. TIME COVERED	14. DATE OF REPORT (Year, Month, Day)	15. PAGE COUNT
In-House	FROM Mar 87 TO Aug 88	November 1989	40

16. SUPPLEMENTARY NOTATION: N/A

17. COSATI CODES			18. SUBJECT TERMS (Continue on reverse if necessary and identify by block number)
FIELD	GROUP	SUB-GROUP	
20	06		Picosecond Pulse Laser, Electro-Optic Sampling, Degenerate Four Wave Mixing, Autocorrelation

19. ABSTRACT (Continue on reverse if necessary and identify by block number)

This report contains the results of our work in setting up, aligning, and characterizing the picosecond pulse laser facility in the Photonics Laboratory of the Rome Air Development Center. It explains the theory of production of picosecond pulses using a dye laser pumped by a mode locked argon laser. It also briefly describes our suggested uses of this facility. These include degenerate four wave mixing for the measurement of nonlinear optical effects in optical materials and electro optic sampling for the characterization of ultrafast electronic and optoelectronic devices.

Keywords

20. DISTRIBUTION/AVAILABILITY OF ABSTRACT: ☐ UNCLASSIFIED/UNLIMITED ☒ SAME AS RPT. ☐ DTIC USERS	21. ABSTRACT SECURITY CLASSIFICATION: UNCLASSIFIED
22a. NAME OF RESPONSIBLE INDIVIDUAL: DOROTHY JACKSON, 1Lt, USAF	22b. TELEPHONE (Include Area Code): (315) 330-4092; 22c. OFFICE SYMBOL: RADC(DCLW)

DD Form 1473, JUN 86 — Previous editions are obsolete. — SECURITY CLASSIFICATION OF THIS PAGE

UNCLASSIFIED

TABLE OF CONTENTS

LIST OF FIGURES

1.0 INTRODUCTION

Future signal processing and computing requirements present an ever increasing demand for speed, bandwidth, and parallelism of systems. Recent developments in electronics technology have pushed electronic systems to their physical limits of speed and bandwidth. However, optical systems promise further advances because, instead of electrons, they use photons which have much higher limits on these parameters. Optical systems also offer the potential for a high degree of parallelism since beams of light do not interfere with each other as electrons do. These possibilities provide a strong motivation for the study of ultrafast optical events in materials and newly emerging devices not only to understand the mechanisms behind these events, but to use this understanding to improve the state of the art.

Recently developed materials and devices exhibit measurable picosecond and even femtosecond optical responses. These include Multiple Quantum Well (MQW) structures, III – V semiconductor compounds, and organic polymers. A picosecond pulse laser facility such as the one at RADC provides the means to test new devices and materials, to validate the performance of devices, and to assist in the design of new material structures which can improve the state of the art.

This report shall describe the picosecond pulse laser facility and related equipment

used in the facility. It will also describe our procedures for setting up, aligning, and characterizing the facility. Finally, it will discuss some possible applications of picosecond pulsing in research and development of materials and devices.

1.1 Equipment

Our facility currently consists of a Spectra Physics 171–09 Argon Ion Laser (18 W all lines output), a Spectra Physics mode locking system with 452A Mode Locker Driver, 453 Mode Locker Stabilizer, and 342A Mode Locker, a Spectra Physics Sync Pumped 375B Dye Laser operating with Rhodamine 6G dye and a Spectra Physics 409 Autocorrelator. All this is mounted on a Newport 16' x 4' Research Series Table Top. We are using a Tektronix 7104 Oscilloscope with 7B10 Time Base and 7A26 Dual Trace Amplifier for autocorrelation measurements, a Tektronix 7S11 Sampling Unit and 7T11 Sampling Sweep with S6 Sampling Head and an Antel Optronics AR–S2 Photodetector for measurements of the Argon Laser's mode locked output.

2.0 Theory of Picosecond Pulse Generation

The method used to generate the picosecond pulses is called synchronous pumping. The dye laser is pumped in synchronism with an actively mode locked argon ion laser. Thus the argon laser and the dye laser interact with each other. This interaction can be explained by first beginning with the mode locking of the argon laser, then by showing how the dye laser is excited by the output of the modelocked argon laser to produce picosecond pulses. The method of measurement of the pulses also is of interest and the use of autocorrelation techniques will be explained.

A laser cavity can support a number of optical frequencies or modes. For a mode locked laser output, these frequencies are separated in the frequency domain by the relationship

$$\omega = \frac{\pi c}{l} \tag{1}$$

and are periodic in time as

$$T = \frac{2l}{c} \tag{2}$$

where l is the length of the laser cavity and T is the round trip transit time inside the cavity. This property arises from the phase relationship of the total optical field, e(t), where

$$e(t) = \sum_n E_n e^{i[(\omega_o + n\omega)t + \phi_n]} \tag{3}$$

where n corresponds to the nth mode, ϕ_n is the phase of the nth mode, and ω_o is some arbitrary frequency. The laser can be mode locked either by shortening the cavity length, l, which increases the mode spacing ($\omega = \pi c/l$) to the point where only one mode can oscillate, or by fixing the phases and amplitudes of the modes to some relative value. The latter mode locking technique is used with our equipment.

The mode locking is achieved by producing losses in the cavity modulated at a frequency which corresponds to the modal spacing. An acousto optic modulator acts as a shutter which is closed most of the time except for a brief opening every $T = 2l/c$ seconds corresponding to the round trip transit time of the cavity.

The acousto optic cell in this application is a crystal made in the form of a prism as

shown in figure 1. A piezoelectric transducer is mounted to an end face of the crystal. When an electrical signal is applied to this transducer it vibrates producing an acoustic wave propagating through the material. This acoustic wave, traveling at the speed of sound in the material, causes a perturbation of the density of the material which, in turn, causes a sinusoidal change in its index of refraction. The acoustic wave travels the length of the material and bounces off the end face back towards the transducer. If the frequency of the applied electrical signal corresponds to a resonant frequency of the acoustic cell the traveling acoustic wave will set up a standing wave pattern in the cell modulating the index of refraction. This appears as a shutter to the laser light that opens periodically for a brief interval. Incident optical beams that have a frequency relationship which corresponds to that of the electrical signal on the transducer will propagate through the cell and not be attenuated.

Either the cavity length of the laser or the acoustic resonance of the acousto optic cell can be adjusted so that the round trip transit time and frequency spacing of the modes in the laser correspond to the applied electrical frequency of the acousto optic cell. This optimizes the efficiency of the mode locking. This optimum condition is described by

$$2f = \Delta\nu = c/2l \tag{4}$$

where f is the center frequency of the acoustic resonance and $\Delta\nu$ is the frequency difference between adjacent longitudinal modes of the laser. The relationship between the cavity length of the laser and the parameters of the acoustic cell are

$$l = \frac{Lc}{2nV} \tag{5}$$

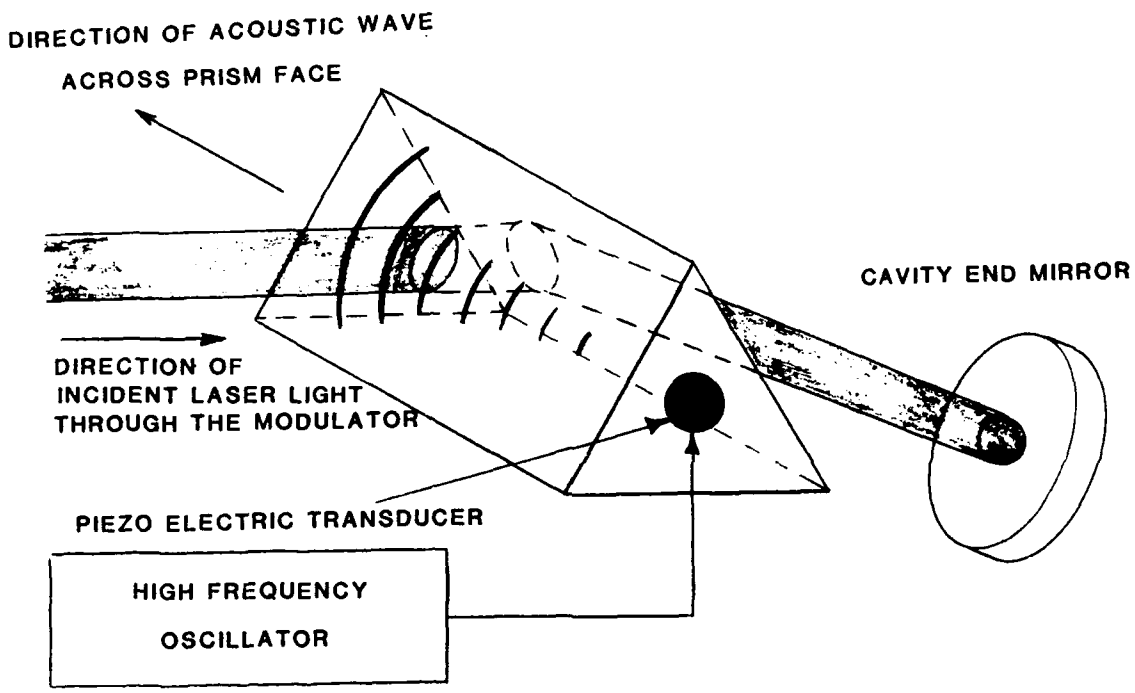

Figure 1. Schematic representation of the acoustic optic modulator used in argon ion laser mode locking.

where L is the length of the acoustic cell, n is the number of acoustic wavelengths in one round trip through the acoustic cell, and V is the acoustic velocity.

Both the acoustic velocity and the acoustic cavity length are temperature dependent so some means of stabilizing the temperature is required, otherwise the acoustic frequency will drift. When electrical and optical power is applied to the modulator it tends to heat the modulator. This heating must be controlled or the resonant frequency of the acousto optic cell will drift away from the driver frequency of the electrical signal resulting in a lowering of coupling efficiency and mode locked laser performance. A stabilizer which feeds back information about drift and automatically adjusts the driver power level can maintain a constant temperature.

The previously described mode locking technique has the effect of locking modes of equal amplitude and phase into a fixed relationship as shown in figure 2. A useful case is when $\phi_n = 0$ in equation (3). For N oscillating modes with equal amplitudes and $E_n = 1$, equation (3) becomes

$$e(t) = \sum_{-(N-1)/2}^{(N-1)/2} e^{i(\omega_o + n\omega)t} = e^{i\omega_o t} \frac{\sin\ (N\omega t/2)}{\sin\ \omega t/2} \tag{6}$$

Then the average laser power output is given by

$$P(t) \propto \frac{\sin^2(N\omega t/2)}{\sin^2(\omega t/2)} \tag{7}$$

The power consists of a trace of pulses with period $T = 2l/c$, as shown in figure 3, corresponding to a pulse occurring for each round trip cavity transit time of the laser. Each mode adds to the amplitude of the pulse. It also can be determined that the

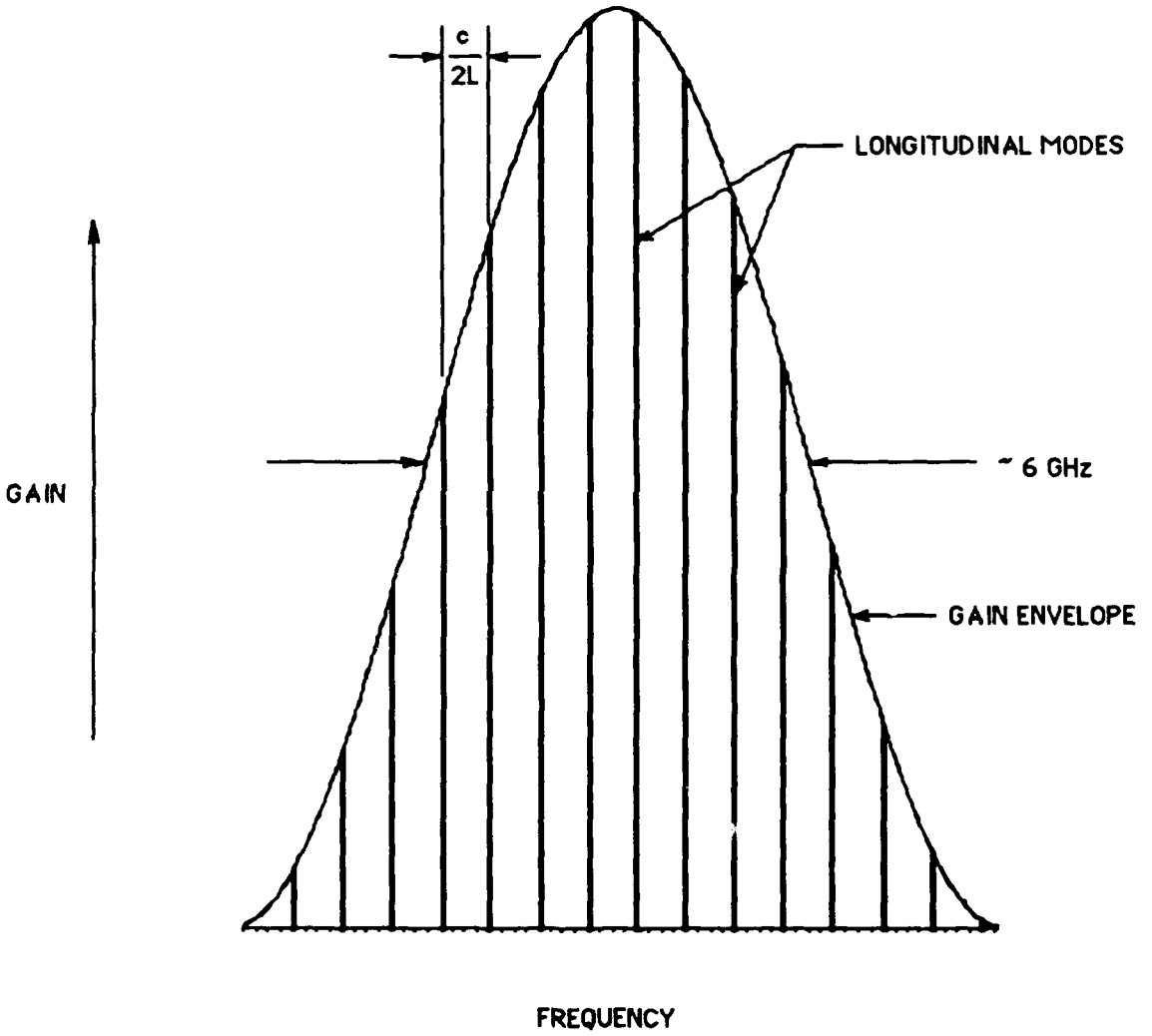

Figure 2. Amplitude, frequency, and phase relationship in a mode locked ion laser.

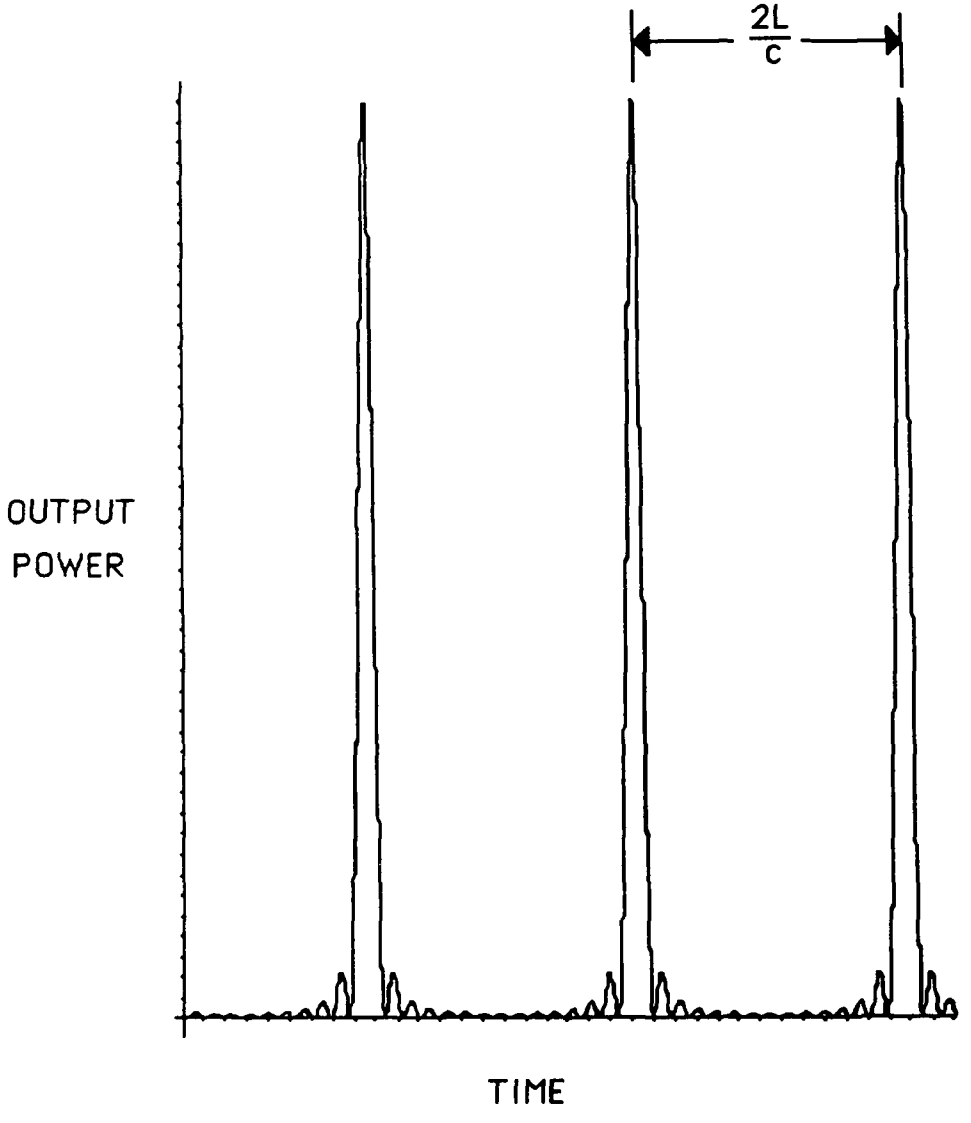

Figure 3. Output of a modelocked laser. This plot was done assuming N = 15 in equation (7).

pulsewidth, τ_o, has the following relationship to the laser linewidth

$$\tau_o \approx .4 \left[\frac{2\pi}{\Delta\omega}\right] = \frac{.4}{\Delta\nu} \tag{8}$$

This shows that the pulsewidth is inversely proportional to the gain linewidth of the laser. The shortest pulses are obtained from mode locked lasers which have a relatively broad linewidth. For the argon laser with a linewidth of 5 GHz, the minumum pulsewidth can be expressed by

$$\tau_o \approx \frac{.4}{5\text{GHz}} = 80 \text{ picoseconds}$$

This also explains why dye lasers are so effective at producing narrow pulsewidths. The linewidth of a dye laser is typically approximately 1000 GHz which is much broader than that of an argon laser. This corresponds to a pulsewidth of approximately 400 femtoseconds that is achievable with this type of laser.

Once mode locking of the argon laser is achieved the dye laser must be aligned and its cavity length adjusted to match that of the argon laser for synchronous pumping to occur. The cavity length of the dye laser is matched to that of the argon laser so that the round trip transit time of a pulse within the dye laser cavity corresponds to that of the argon, or other, pump laser. In this way, the modal frequency spacing of the dye laser is a multiple of that of the pump laser. This synchronization causes the gain medium of the dye laser to be excited in such a manner that the argon pumping pulse and the mode locked pulse of the dye laser arrive simultaneously and overlap spatially and temporally in the dye stream. The longer pumping pulse of the argon laser brings the population of the dye up to its threshold value which is the point where a population inversion exists. The dye laser

pulse arrives at the jet stream of the dye just as this threshold is reached and rapidly depletes the population. This results in a much shorter pulse than the pump pulse. This is illustrated in figure 4.

As mentioned before, the short pulsewidths of the dye laser are a function of the linewidth of the dye laser. The broad linewidths of dye lasers allow them to be tuned over a much wider range of wavelengths than many other types of lasers with the exception of Ti Sapphire lasers. Several different types of tuning elements are available. Tuning wedges and birefringent filters can be used in this dye laser. These are illustrated in figure 5. A tuning wedge consists of two mirrors separated by a wedge shaped material. As this wedge is slid across the path of the optical beam the distance the beam must travel between the mirror surfaces changes and the allowable frequencies resonant in the cavity shift as well, thus changing the output wavelength. The output linewidth of a tuning wedge is approximately 240 GHz corresponding to τ_o = 1.7 picosecond pulsewidths. A birefringent filter is the type we used in our picosecond pulse system. Birefringent filters consist of one or more quartz plates which exhibit birefringence. The filter is oriented at Brewster's angle within the laser cavity. The plates are cut so that their optical axes are parallel to their surface. A plate of thickness, t, will introduce a phase difference, σ, between the polarized transmitted waves of

$$\sigma = \frac{2\pi}{\lambda} d(n_o - n_e) \tag{9}$$

where n_o and n_e are the refractive indices of ordinary and extraordinary rays, respectively. This birefringence causes the linearly polarized incident laser beam to become elliptical. As the previous equation suggests, there is a dispersion relationship between wavelength and phase shift, hence, wavelength selectivity arises because only certain wavelengths can

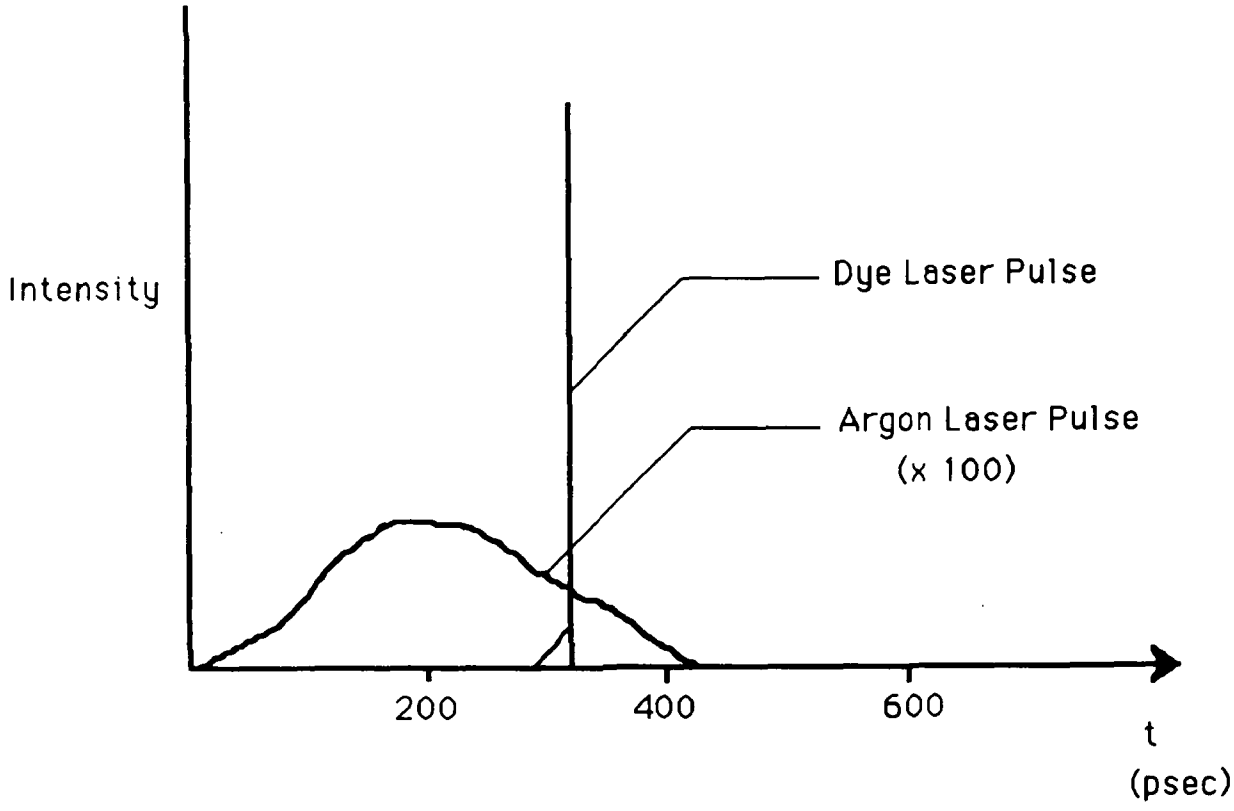

Figure 4. Pulse shortening in the synchronous pumping process.

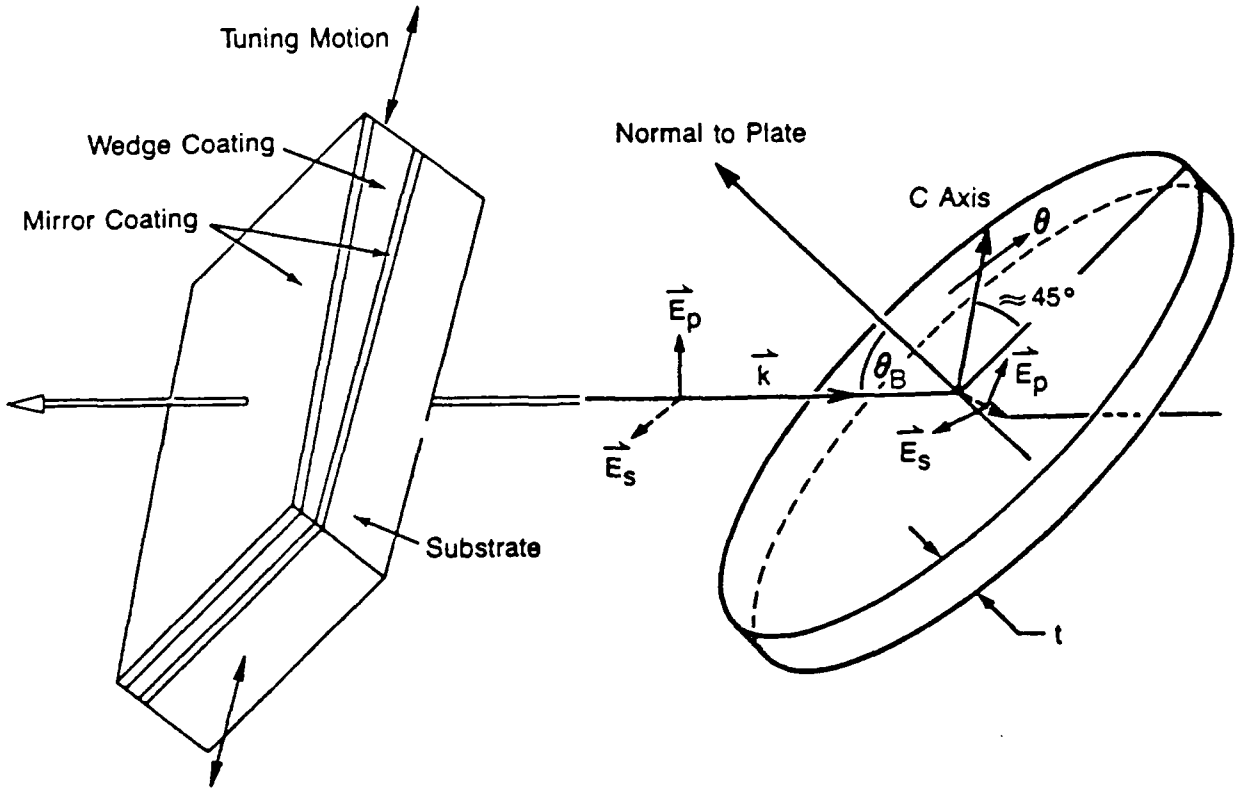

Figure 5. Tuning wedge and birefringent filter designs.

make a complete π polarization shift. All other wavelengths will be deflected at angles which will cause them to suffer losses at the dye stream and fail to reach the lasing threshold. Tunability of the birefringent filter comes as a result of rotating the filter about an axis that is normal to the plates. This will vary the wavelengths that are allowed to pass through the plates. The birefringent filter typically has a range of tunability between 80 and 100 nanometers. When additional birefringent plates are added the selectivity of a particular wavelength is increased. This selectivity is referred to as finesse and is determined as shown in figure 6.

However, this decreases the linewidth of the dye laser which also has the effect of increasing the pulsewidth. With a two plate filter the linewidth becomes less than 60 GHz corresponding to a pulsewidth of 6.6 picoseconds. For three plates the linewidth becomes less than 40 GHz corresponding to a pulsewidth of 10 picoseconds.

When all the aforementioned parts; argon laser, modelocker, and dye laser, are working properly, pulses of from 1.5 to 3 picoseconds are produced. These pulsewidths are beyond the capability of most currently available direct methods of measurement. The method used in our case is based on obtaining an autocorrelation trace using a nonlinear process called second harmonic generation in a Michelson interferomenter configuration. This method can be described by considering figure 7. A mode locked pulse from the dye laser is divided by a beam splitter into two pulses of equal intensity, one of which is delayed with respect to the other. The following equations describe this situation

$$e_1(t) = E(t) \cos \omega t \tag{10}$$

$$e_2(t) = E(t - \tau) \cos \omega(t - \tau) \tag{11}$$

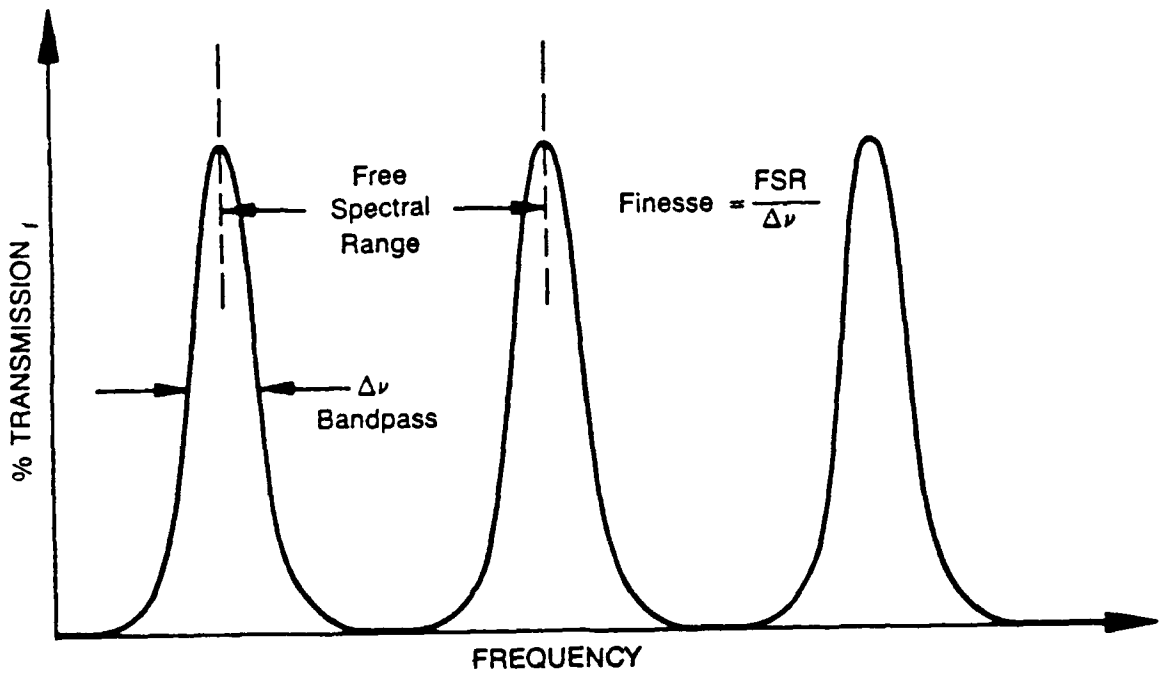

Figure 6. Etalon Frequency transmission characteristics.

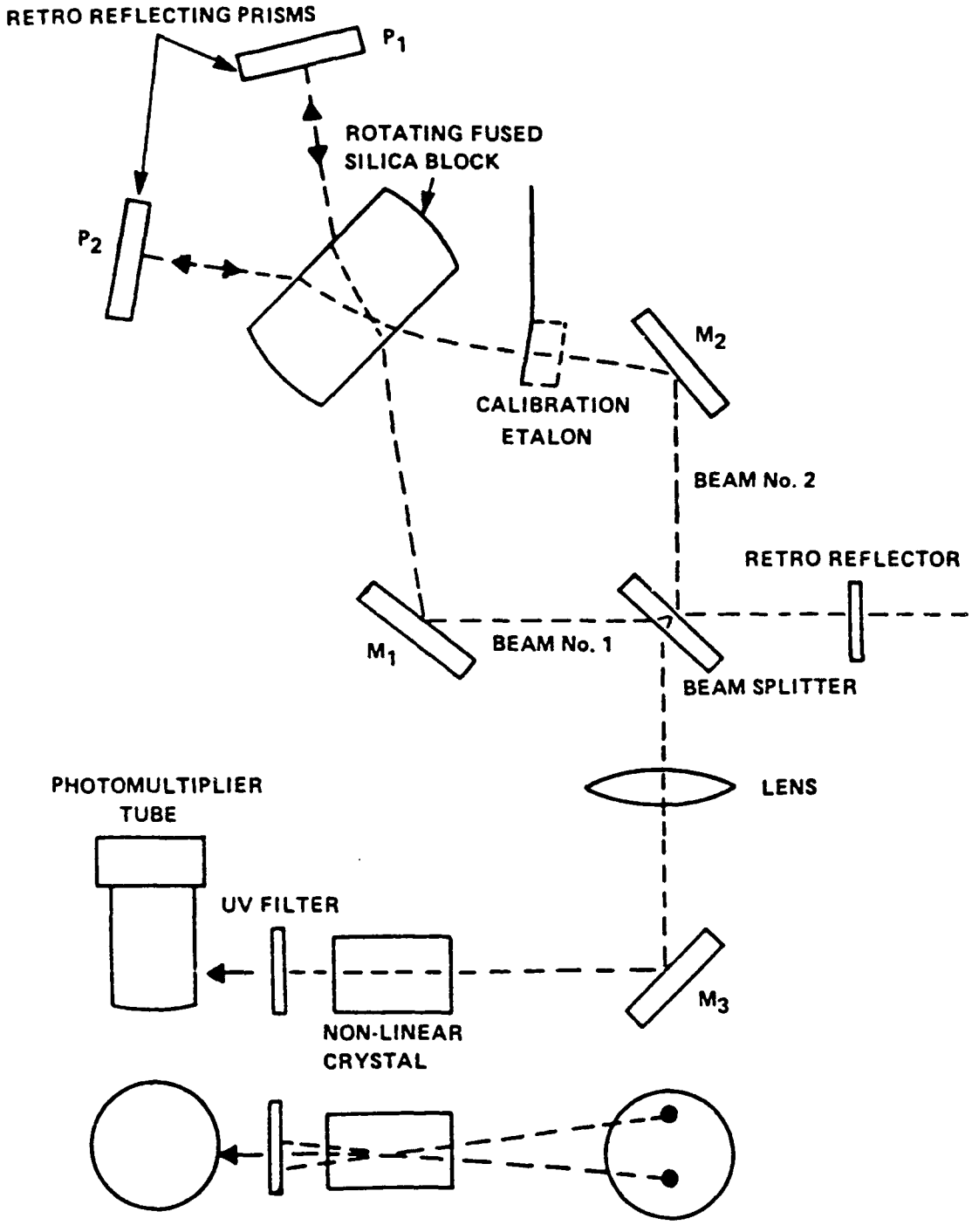

Figure 7. Autocorrelator internal beam path configuration

The delay is accomplished by a variation in path length induced by a rotating block of silica The two beams enter the block at complementary angles, θ and ϕ, to the normal of the block surface. As the block rotates, the variation in optical path length as a function of the incident angle is given by

$$l(\theta) = L + t\left[\sqrt{n^2 - \sin^2\theta} - \cos\theta\right] \tag{12}$$

where L is the path length of the beam outside of the block for $\theta = 0$, n is the index of refraction of the block, and t is the thickness of the block. A similar expression holds for the complementary angle ϕ. However, since it is complementary to θ it decreases as θ increases.

$$l(\phi) = L - t\left[\sqrt{n^2 - \sin^2\phi} + \cos\phi\right] \tag{13}$$

The relative change in path length or delay induced is given by the difference between these expressions.

As the block rotates the pulses will move together and overlap at the point where the angle for both pulses is such that the path lengths are the same. Thus, the intensity of the optical beam is a function of the correlation function between the recombining pulses which is directly related to their pulse width. The two pulses are then incident on a nonlinear optical crystal such as KDP. This crystal produces a second harmonic pulse. According to theory, the amplitude of the second harmonic is proportional to the square of the incident optical field.

$$\xi(t) = (e_1(t) + e_2(t))^2 = e_1(t) + 2e_1e_2(t) + e_2(t)^2 \tag{14}$$

This second harmonic signal is then incident on a photomultiplier tube or other "slow" detector. Its output voltage is the integrated intensity of the second harmonic over a time, T, that is long compared to the optical pulse duration. A filter blocks the fundamental frequency and intensity is the square of the optical field. Equations which describe this situation are

$$V(t) = \frac{1}{T}\int_{-T/2}^{T/2} \xi(t)^2 dt \tag{15}$$

for

$$I = \xi(t)^2 = e_1^4 + e_2^4 + 6e_1^2e_2^2 + 4e_1^3e_2 + 4e_1e_2^3 \tag{16}$$

where

$$\frac{1}{T}\int_{-T/2}^{T/2} e_1^4 dt = \int_{-T/2}^{T/2} e_2^4 dt = \int_{-T/2}^{T/2} E^4(t)dt \int_{-T/2}^{T/2} \cos\omega t dt = \frac{3}{8}\int_{-T/2}^{T/2} E^4(t)dt$$

and

$$\frac{6}{T}\int_{-T/2}^{T/2} e_1^2e_2^2 dt = \frac{6}{T}\left\{\int_{-T/2}^{T/2} \frac{1}{4}(1+\cos 2\omega t)[1+\cos 2\omega(t-\tau)]dt\right\} \int_{-T/2}^{T/2} E(t)^2E(t-\tau)dt$$

$$= \frac{3}{2} \int_{-T/2}^{T/2} E^2(t)E^2(t-\tau)dt$$

The odd powered terms, $4e_1e_2^3$ and $4e_1^3e_2$, average to zero when integrated. Therefore,

$$V(t) = \frac{3}{4}\int_{-T/2}^{T/2} E^4(t)dt + \frac{3}{2}\int_{-T/2}^{T/2} E^2(t)E^2(t-\tau)dt \tag{17}$$

where the term

$$\frac{3}{2}\int_{-T/2}^{T/2} E^2(t)E^2(t-\tau)dt$$

is the autocorrelator function of the intensity envelope of the light pulse. If we define $G(\tau)$ as

$$G(\tau) = \int_{-T/2}^{T/2} \frac{E^2(t)E^2(t-\tau)dt}{E^4(t)dt} \tag{18}$$

then

$$V(t) = \frac{3}{4}\int_{-T/2}^{T/2} E^4(t)dt[1+2G(\tau)] \tag{19}$$

where

$$\frac{3}{4}\int_{-T/2}^{T/2} E^4(t)dt$$

is not a function of τ and thus represents only a background DC voltage we'll call V. When no autocorrelation is present, ie $G(\tau) = 0$, then $V(t) = V$. When the pulses are overlapping and autocorrelated, $G(\tau) = 1$ and $V(t) = 3V$. So a plot of V(t) versus τ will consist of a peak of height 3 against a background of height 1. The peak will have a width proportional to the pulsewidth. The relationship of the actual pulsewidth to pulse shape is a function of the type of waveform observed. A gaussian pulse defined by

$$V(T) = \exp\left[\frac{-(4\ln 2)t^2}{\tau_o^2}\right] \tag{20}$$

will have a relationship between the actual pulsewidth, τ_o, of $t/\tau_o=\sqrt{2}$ so $\tau_o=.7t$. Whereas a transform limited pulse defined by

$$V(T) = \exp\left[\frac{-(\ln 2)t}{\tau_o}\right] \tag{21}$$

will have an actual pulsewidth, τ_o, related by $\tau_o=.5t$.[1]

3.0 Experimental Procedures

We achieved successful modelocking of the argon laser which produced approximately 150 picosecond pulsewidths at 900 mW output power. This procedure was extremely touchy. It was difficult to maintain a consistent rf frequency match with that

of the laser cavity. This may have been caused by problems with the 342A mode locker or changes in the ambient temperature of the air in the room. We found that the mode locker was somewhat loose in its mounting and corrected this problem. We had an additional problem with the cooling water into the argon laser. The setup that we had was very sensitive to pressure drops from outside sources. A more accurate means of regulating water pressure was needed to replace the simple pump and pressure regulator we had installed. We eventually switched over to a closed loop water chiller system.

After mode locking was achieved and output power was maximized we aligned the argon laser with the dye laser and adjusted the cavity of the dye laser to match. Using a two plate birefringent filter and R6G dye we were able to achieve 300mW of output with a pulsewidth of 2.0 picoseconds with 5% sidelobes. Figure 8 is a photograph of one of our pulse shapes. The calibration factor of the oscilloscope is measured by inserting a calibration etalon in the path of one of the beams of the autocorrelator. This will produce a shift in the o'scope trace corresponding to a delay of Δt where

$$\Delta t = \frac{(n-1)\ 13.15mm}{c} \tag{22}$$

where n is the index of refraction of the etalon, 13.15 mm is the thickness of the etalon, and c is the speed of light. Therefore,

$$\Delta t = \frac{(.456)(13\ .\ 15mm)}{3\ x\ 10^{11} mm/sec} = 20 \text{ picoseconds.}$$

The autocorrelation width is measured by taking the ratio of this delay to the actual number of divisions shifted on the o'scope, then applying this calibration factor to the measured full width at half maximum (FWHM) of the pulse on the o'scope, ie

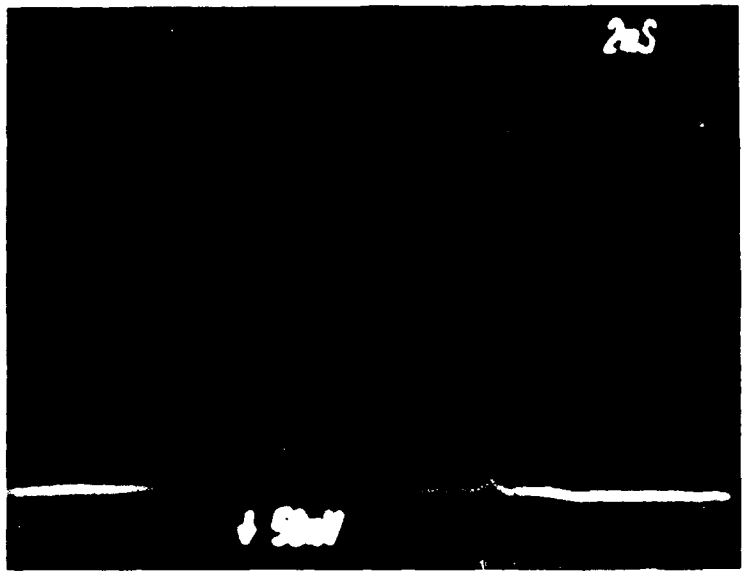

50mV/2ms

Figure 8. Photograph of the picosecond pulsed laser's output. Assuming a Gaussian pulse shape, the pulsewidth at full width half maximum (FWHM) was measured to be 3.1 picoseconds.

$$\text{Autocorrelation width} = \frac{20.0 \text{ psec}}{6.8 \text{ subdivisions of shift}}(1.5 \text{ subdivisions at FWHM})$$

$$= 4.41 \text{ psec.}$$

The pulse shape that you assume will determine the actual pulse width. The autocorrelation trace does not provide any details about the actual pulse shape. The relationship between the pulse shape and the actual pulse width varies depending on the pulse shape assumed. If you assume a transform limited single sided exponential, as shown in figure 9b, the decorrelation factor is .5 for this pulse shape. Therefore, the actual pulsewidth would be 2.2 psec. If you assume a Gaussian shaped pulse, as shown in figure 9a, the decorrelation factor would be .7; thus, the pulsewidth would be 3.1 picoseconds.

4.0 Applications of Picosecond Pulse Equipment

This section will explore possible uses of the picosecond pulse facility in the development of materials and devices. Time resolved measurements of nonlinear optical effects, measurements of electrical dispersion in transmission lines, photodetector characterization, ultrafast transistor characterization, and noncontact testing of GaAs integrated circuits are just a few of the uses that are possible for this system.

4.1 Characterization of Nonlinear Optical Materials

This picosecond facility is suitable for the temporal characterization of nonlinear optical materials. The third order nonlinear optical susceptibility, χ^3,can be measured with pulses of suitably high peak powers. The χ^3 parameter is related to the intensity

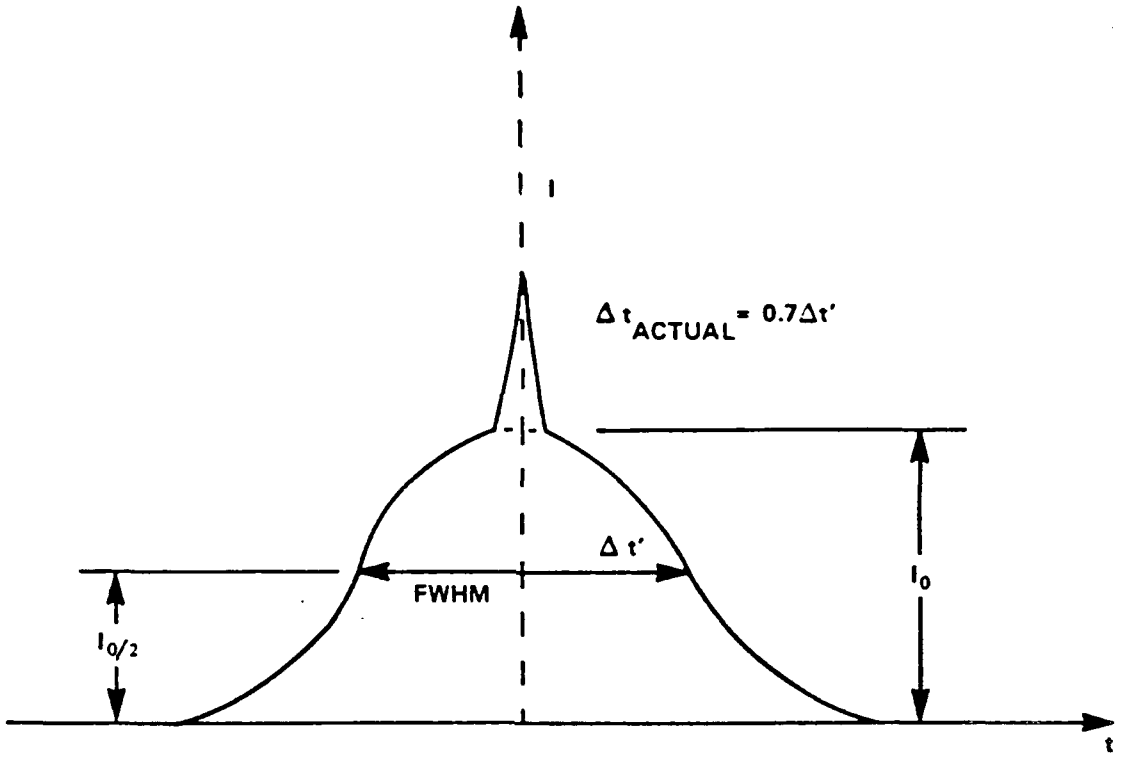

Figure 9a. Non-Transform-Limited Gaussian Pulse

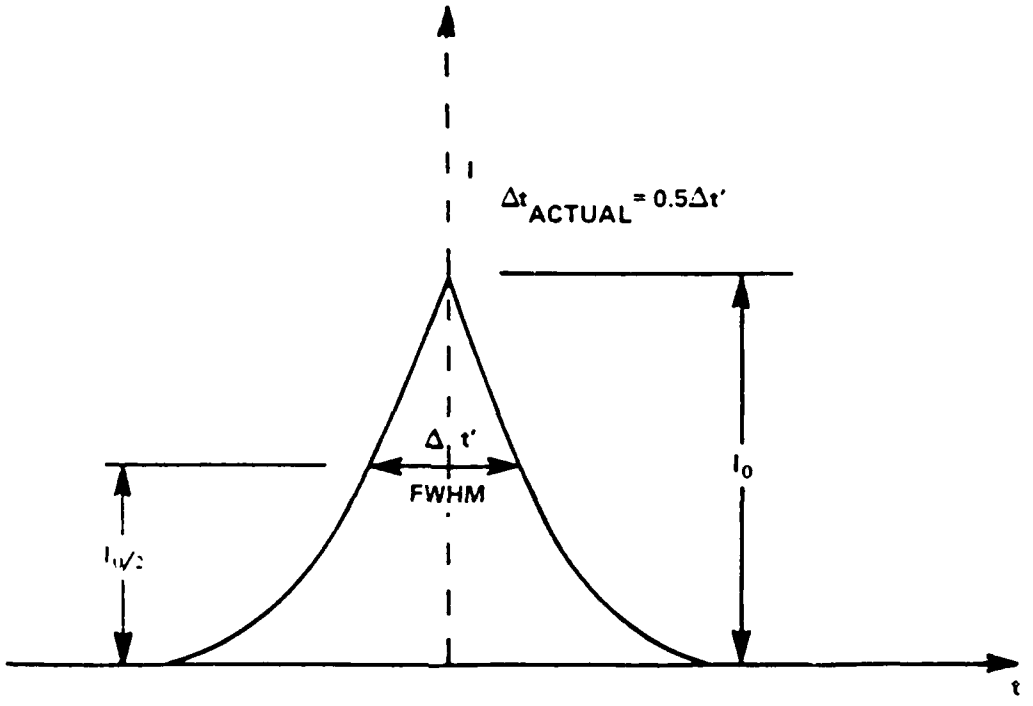

Figure 9b. Transform-Limited, Single Sided Exponential Pulse

dependent refractive index of a material. It determines how readily the refractive index of the material will vary upon the application of an optical signal. This parameter is important to the use of these materials as all optical switches and logic devices. $\chi^3(\omega)$ is the quantity that describes the change in dielectric constant, ϵ_1, with optical intensity. The dielectric constant, ϵ, of an isotropic material (one that has the same properties in all directions) can be described by

$$\epsilon = \epsilon_1 + 4\pi\chi^3|E|^2 \tag{23}$$

where ϵ_1 is the linear dielectric constant and E is the optical field. This relates to the expression for the intensity dependent index of refraction of a material, ie

$$n = n_1 + n_2 I \tag{24}$$

where n is the linear index of refraction and I is the optical intensity, through the coefficient n_2 defined by

$$n_2 = 16\frac{\chi^3}{\pi^2 c\epsilon_1} \tag{25}$$

In organic materials the χ^3 nonlinearity is due primarily to electronic effects at nonresonant frequencies and can have an extremely fast response time in the femtosecond regime.

χ^3 effects can be determined by using a degenerate four wave mixing (DFWM) scheme as shown in figure 10. Three incident beams with a common frequency, ω, interact

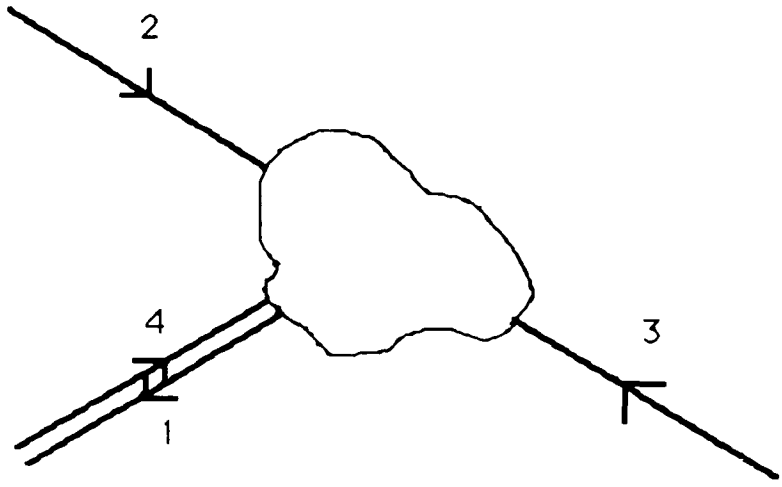

Figure 10. Degenerate four wave mixing. All beams are of the same frequency.

in the medium creating a fourth beam. Beams 2 and 3 are counterpropagating pump beams. The probe beam, labelled 4, overlaps the pump beams at any arbitrary angle. The generated signal beam, 1, will have the same frequency, ω, as the incident beams and will be the phase conjugate of the probe beam.

An experimental arrangement for measurement of χ^3 by DFWM is shown in figure 11. There are a number of constraints necessary in order to realize efficient phase conjugate reflectivity.[2] First, the source laser should operate in a single longitudinal and transverse mode. This maximizes the laser coherence length, thus enabling one to use longer interaction lengths as well as relaxing path length difference constraints. The pump waves should be nearly planar and spatially filtered for efficient and precise conjugation. The source laser must be isolated from the experimental apparatus; retroreflection of the beams back into the laser may affect its mode properties and/or coherence characteristics. The propagation directions of the two pump beams must be antiparallel to optimize the conjugate reflection coefficient, R. Also, the temporal overlap of the three pulses in the nonlinear medium must be maximized for efficient phase conjugate generation. This is accomplished by the adjustment of the optical delay lines. Care must also be taken with respect to the ratio of the amplitudes of the pump beams, ξ_f/ξ_b, and to the maximum pump beam intensity. Also of significance is the probe to pump beam amplitude ratio. Calibration of the DFWM signal for measurement of the DFWM reflectivity, R, is usually done by removing the nonlinear medium and inserting a 100% retroreflector in the path of the probe beam.

The magnitude of χ^3 is estimated by measuring the signal to probe reflectivity, R, as a function of the interaction length in the nonlinear medium and of $\sqrt{I_f I_b}$, where I_f and I_b are the intensities of the forward and backward pumps, respectively. Then, for low reflectivities and low material absorption coefficients, χ^3 can be estimated from the

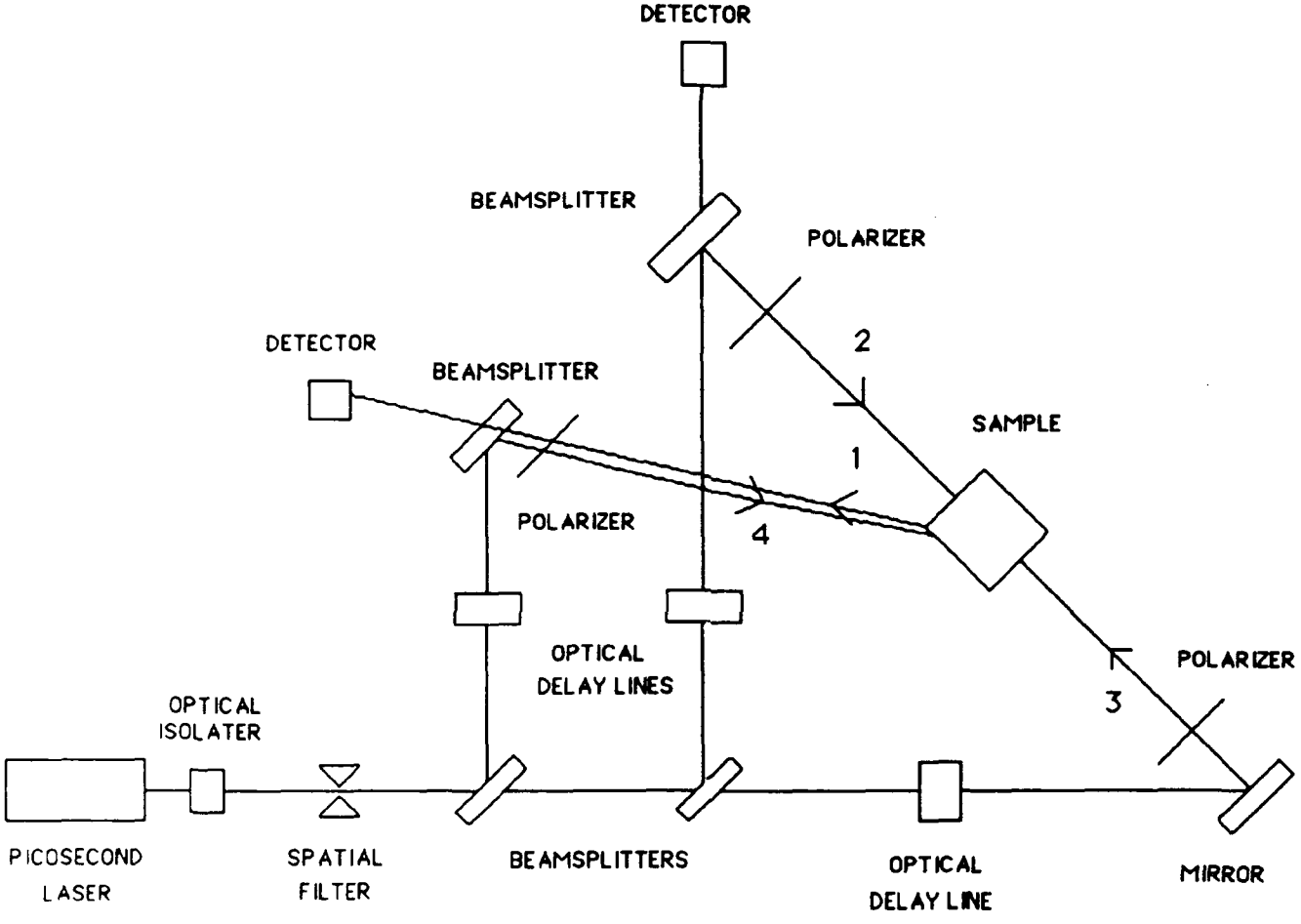

Figure 11. Schematic of degenerate four wave mixing (DFWM) setup. Beams 2 and 3 are counterpropagating pump beams. Beam 4 is the probe beam. Beam 1 is the generated phase conjugate of the probe beam.

expression

$$R = |\kappa|^2 L^2 \tag{26}$$

where

$$\kappa = (2\pi\omega/nc)\chi^3 \xi_f \xi_b \tag{27}$$

and L is the interaction length in the nonlinear medium. For absorbing samples, one must consider the attenuation of the beams as they propagate through the sample. The reflectivity, R, versus $\sqrt{I_f I_b}$ equations of Yariv and Pepper[3] and AuYeung et al[4] can be used to estimate the magnitude of χ^3 from the linear portion of the lnR vs ln $\sqrt{I_f I_b}$ plot.

4.2 Electro Optic Sampling

The electro optic sampling technique can be used to measure a variety of effects. This technique is useful where ultrafast electrical pulses suitable to characterize electronic and optoelectronic devices and circuits are difficult, if not impossible, to generate by any other means.

Figure 12 shows the layout of an electro optic sampling system.[5] The optical pulse train of a picosecond laser system is split into two beams. One beam triggers the generation of an electrical signal which is to be measured. The other beam samples the field induced birefringence in the electro optic medium due to the electrical signal. The electrical signal can be generated by a photosensitive device which converts the picosecond optical pulses into electrical energy. The sampling optical beam is passed through a delay

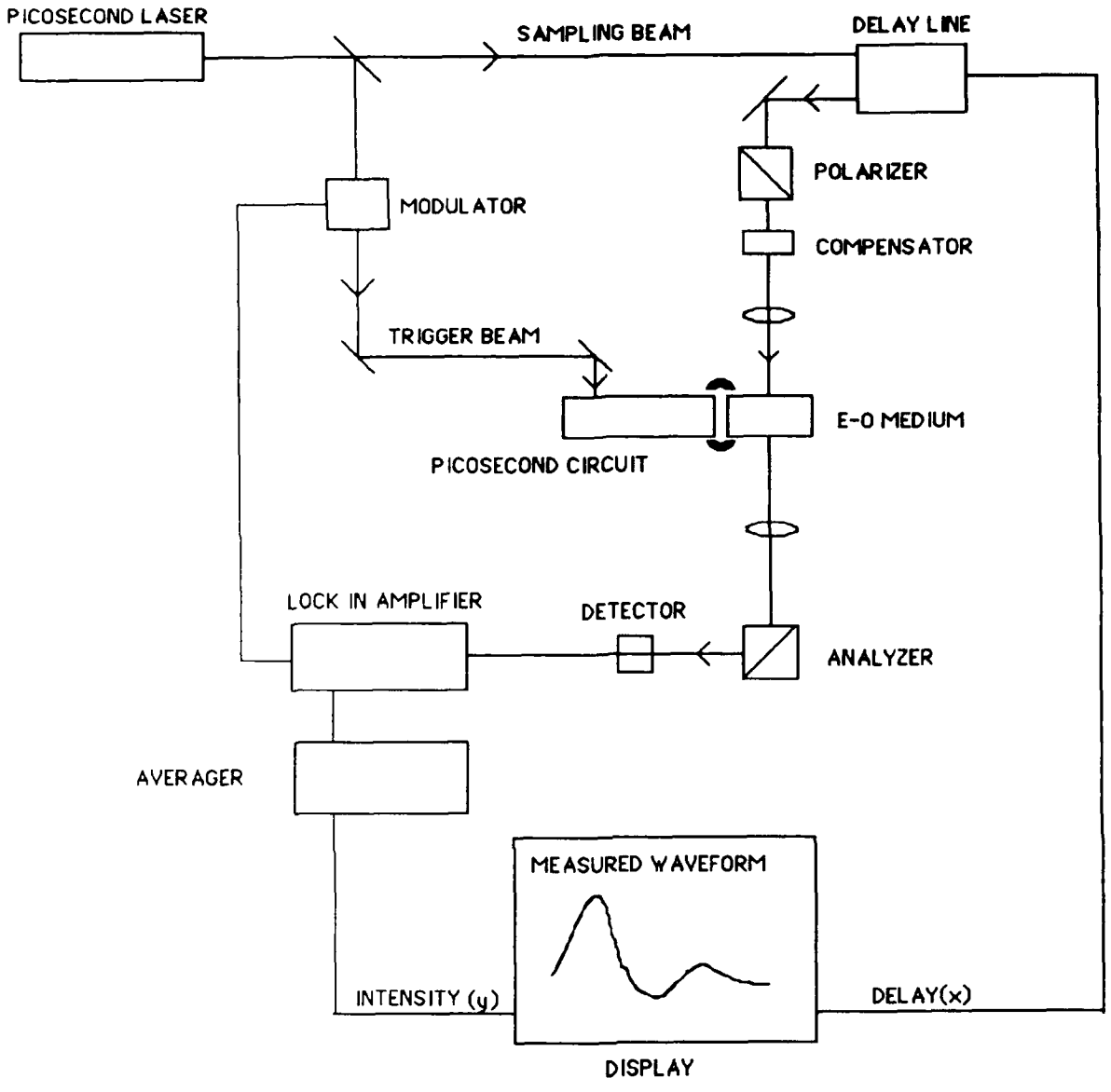

Figure 12. Electro Optic Sampling system. Pulses from the picosecond laser system are split up into two beams. The trigger beam generates the electrical signal from the circuit to be characterized. The sampling beam travels through Electro optic medium which has been modulated by the previously generated electrical signal

device which synchronizes it with a display device for scanning. This sampling pulse is then focused onto the electro optic medium. The electro optic medium is modulated by the electrical signal previously generated in the trigger beam. This, in turn, modulates the intensity of the sampling beam corresponding to the amplitude of the electrical signal. A lockin amplifier measures the amplitude of the modulated optical signal giving a time representation of the electrical signal under study.

This technique can be applied to the measurement of dispersive effects in stripline electrodes. This dispersion is a function of the dielectric constant of the material and of the specific electrode geometry. These effects can be considerable for high frequency operation and may not be measurable with state of the art electronic equipment. This measurement technique can aid considerably in the design and characterization of new materials such as superconductors and the optimization of electrode geometries for specific high frequency applications.

The electro optic sampling technique can also be applied to the characterization of photodetectors, ultrafast transistors (MODFET) and noncontact testing of GaAs integrated circuits.

5.0 Summary and Conclusions

In short, we have set up a picosecond pulse laser facility in the Photonics Laboratory. We have examined the theory and have made some experimental measurements to characterize the optical output of the laser. We recommend that the picosecond pulse laser be used to perform characterization of high speed nonlinear optical effects and electro optic sampling for characterization and optimization of electronic and optoelectronic devices and circuits.

REFERENCES

1. Spectra Physics manuals for the 375B Dye Laser, 342A Mode Locking System, and 409 Autocorrelator.

2. D. Pepper and A Yariv, Optical Phase Conjugation, Academic Press, Inc , Orlando Florida, 1983, pages 61 – 62.

3. A. Yariv and D. Pepper, Optics Letters, Vol 1, No 1, July 1977, Pages 16 – 18.

4. J. AuYeung et al, Optics Letters, Vol 4, No 1, Jan 1979, pages 42 – 44.

5. J. Valdmanis and G. Mourou, Laser Focus/ Electro Optics, Feb 1986, Pages 84 – 96.